Proceedings World Geothermal Congress 2015
Melbourne, Australia, 19-25 April 2015

Measuring Techniques for in Situ Measurements of Thermodynamic Properties of Geothermal Water

Elisabeth Schröder*, Klaus Thomauske, Jens Schmalzbauer and Sabrina Herberger

Karlsruhe Institute of Technology, IKET, Hermann-von-Helmholtz-Platz 1, 76344 Eggenstein-Leopoldshafen

elisabeth.schroeder@kit.edu

Keywords: Heat capacity, viscosity, density, flow calorimeter, flow viscometer, geothermal water properties.

ABSTRACT

The energy content of geothermal water flow is determined by the chemical and physical water properties and the special flow conditions on site, like mass flux, temperature and pressure. For dimensioning geothermal power plants and/or district heat systems, energy content of the brine is the most important parameter. Flow rate, temperature and pressure measurements are common but determination of thermodynamic water properties at power plant operating conditions is often uncertain. High amounts of dissolved minerals and gases influence the water properties significantly. Sample taking of geothermal water and measuring of the physical properties in the laboratory tends to lead to big errors if temperature and pressure level cannot be kept constant. Gasification and/or precipitation of minerals might occur which change the fluid properties substantially.

Against this background a measuring technique was developed and installed which allows for identifying the main thermodynamic properties of the brine on site in a bypass line of the pipe system. The mobile configuration consists of a flow calorimeter for isobaric heat capacity determination, a capillary viscometer for kinematic viscosity ascertainment, and a density measuring device. All components are our own developments and are tested for water and aqueous salt solutions. The accuracy of heat capacity measuring technique amounts to less than 1 per cent based on literature data, the uncertainty of the kinematic viscosity measurements is within a range of 1-2 per cent. All measuring units operate in a temperature range of 0-170°C and pressures up to 30 bar. In addition to our own developments a commercial measuring technique for thermal conductivity determination is appended.

Heat capacity, kinematic and dynamic viscosity, density and thermal conductivity of geothermal fluids can now be determined at geothermal sites as either single point measurement under stationary operating conditions or as multi-point measurement at different temperatures and/or pressures. Detailed knowledge of these fluid properties will serve for a better dimensioning of power plant components, e.g. heat exchangers.

1. INTRODUCTION

The economic efficiency of geothermal power plants depends on many factors of influence. Dominating part are the high costs for drilling, which amount to more than 50% of the total project costs, Finger and Blankenship (2010). For this high efficiency of the power plant is required which means low investment and operating costs and high output of electricity and/or heat. Both aspects are related to the energy content of the geothermal water flow which is determined by mass flow, specific heat capacity and water temperature. Imprecise knowledge of geothermal water properties, e.g. isobaric heat capacity, leads to inexact knowledge of geothermal water heat content and thus to inexact knowledge of heat input to geothermal power plants. Gross and net energy output of the power cycle depends on heat input and thus on heat content of geothermal water flow. For instance if heat input from geothermal water decreases, gross and net energy output of the power cycle similarly decrease. This finding results from calculations with the thermodynamic in-house computer code GESI which allows for efficiency analysis of Organic Rankine Cycles (ORC), Vetter, et al. (2013). Isobaric heat capacity of geothermal water for example, differs from pure water data as a result of mineralization and gas content. Dissolved salt components and gases lead to decreasing heat capacity, as discovered by Thurmond and Brass (1988), Smith-Magowan and Wood (1981) and Hnědkovský, et al. (2002) on binary mixtures of water and sodium chloride. The same effect can be discovered at aqueous solutions of calcium chloride and magnesium chloride as reported by Perron, et al. (1981). The influence of dissolved gases on heat capacity of water is calculated with the computer program REFPROP, Lemmon, et al. (2010) which uses the NIST database. Due to the fact that CO_2 is, besides N_2 and CH_4, the main gas component in geothermal water, Schröder, et al. (2007), a binary mixture of water and CO_2 was regarded. A significant reduction of heat capacity in the order of 5% occurs at gas concentrations of $m_{CO2}/m_{water} = 0.1$.

Besides determining the heat balance of the power cycle, physical fluid properties influence heat transfer within heat exchangers. Heat transfer from geothermal water to the power cycle working fluid within the heat exchanger is determined by heat capacity, kinematic viscosity, density and thermal conductivity of both geothermal water and working fluid. Therefore inaccurate data of isobaric heat capacity can lead to a wrong heat exchanger size. Consequently, heat exchangers that are designed based on pure water data would have an unnecessarily large heat transfer area. For example, calculations with heat exchanger programs, Schröder, et al. (2014) show that a reduction of water heat capacity of 15% leads to reduction of required heat transfer area of 30%.

Kinematic viscosity and density are of minor influence on the heat transfer area if the water flow within the heat exchanger is laminar. The dependence of kinematic viscosity on mineralisation is reported in Kestin, et al. (1981a), Kestin, et al. (1981b) and Xu and Pruess (2001). Their studies on aqueous sodium chloride solutions show, that kinematic viscosity increases with increasing salt content and decreases with rising temperature. Xu and Pruess (2001) investigated as well the influence of sodium chloride on fluid density. They showed that salt components enhance fluid density. In order to estimate the influence of dissolved gases on water

density, calculations with binary mixtures of water and carbon dioxide (CO_2) were made using REFPROP, Lemmon, et al. (2010). The results indicate that increasing gas content leads to decreasing fluid density.

Besides heat capacity, heat conductivity of the brine influences heat exchanger area to a large amount. Reduction of heat conductivity of 10% resulting from water mineralization leads to enhancement of heat transfer area of 4% as calculated with heat exchanger programs, Schröder, et al. (2014). The dependence of heat conductivity of pure water and seawater on mineralization was investigated by Sharqawy (2013). He showed that heat conductivity of seawater decreases with increasing mineral content and increases with rising temperature.

Against the background of dimensioning geothermal power plants, in particular heat exchangers, knowledge of isobaric heat capacity and heat conductivity is essential. In order to determine these physical properties of geothermal water, measuring instruments were built and installed in a mobile setup for performing measurements at geothermal sites under operational conditions. Initial measurement results of specific heat capacity, kinematic viscosity and density of both water and sodium chloride solutions are presented in this paper.

2. INSTRUMENTS OF MEASURE

A test facility is constructed which contains three different measuring instruments for the determination of isobaric heat capacity, kinematic viscosity and density of geothermal fluids. The test facility is constructed as a mobile setup which can be connected to the pipe system of geothermal power plants. The instruments will be used alternatively and temperature and pressure are controlled and kept constant within this setup. Heat conductivity of geothermal water is measured by a commercial instrument (Lambda 1, F5 Technology). This instrument is an offline device but can be filled with geothermal water under in situ pressure and temperature conditions. Measurement results provided by this instrument are not presented within this article. The measuring instruments for isobaric heat capacity, kinematic viscosity and density were tested in the laboratory and are described below.

2.1 Calorimeter

The flow calorimeter consists of a tube which has an inner diameter of 16 mm and a tube length of 735 mm. It is made of PEEK (polyetheretherketone), a low heat conducting material with a high chemical and mechanical resistance. Inside of the tube, two probe heads are installed one at the tube inlet and one at the tube outlet. The inlet probe head consists of a static mixer, four 0.5 mm, NiCr/Ni thermocouples which are distributed radially and an electric heating rod. The length of the rod amounts to 700 mm and is divided into a cold and a hot part. The outlet probe head is configured in the same way as the inlet probe except the heating rod. The hot part of the heating rod at the inlet probe head is 200 mm long and has an outer diameter of 2 mm. The inner wire of the hot part consists of nickel chromium alloy (80/20) whereas the cold part is made of nickel. Both parts of the wire are surrounded by a nicrofer 1.4550 mantle. The rod is installed in the way so that the hot part is located between the thermocouples of both the inlet probe head and the outlet probe head. The PEEK tube is surrounded by a metal tube and the gap between the PEEK tube and the metal tube is evacuated. Additionally insulating material is surrounding the metal tube. This arrangement allows for reducing heat loss. The fluid enters the PEEK tube at the inlet and passes the static mixer which homogenizes the fluid thermally before it passes the thermocouples of the inlet probe head. Here the entrance temperature of the fluid is recorded by the four thermocouples. If the mixer works well no radial temperature fluctuations can be detected. Further downstream the fluid is heated by a constant heat flux which is emitted from the hot part of the electric heating rod. As a result of this heat supply the fluid temperature rises. After homogenization by the static mixer of the outlet probe head the fluid temperature is measured by the four outlet thermocouples. The isobaric heat capacity can now be calculated using following equation:

$$c_P = \frac{\Delta \dot{Q}}{\dot{m} \cdot \Delta T} \tag{1}$$

Where $\dot{m}$ is the mass flux of the fluid which passes the calorimeter, ΔT is the temperature difference which occurs between the inlet and outlet probe heads and $\Delta \dot{Q}$ is the heating power of the rod which is released between the probe heads. The accuracy of the method strongly depends on the accuracy of the power and the mass flux determination. The mass flux is measured by collecting the fluid on a balance (Sartorius, LP34000P) downstream of the calorimeter as function of time. More difficulties arise in the determination of the heating power. Both parts of the heating rod, the hot and the cold part, have electrical resistances which cause heat release. Only the heat released from the rod part which is located between the probe heads is relevant. The heating power of this part is calculated by estimating the electrical resistance from the rod materials and the rod dimensions. For each heating period the electrical current is measured. The heating power is then calculated as follows:

$$\Delta \dot{Q} = R \cdot I^2 \tag{2}$$

Where R is the electrical resistance of the heating rod part which is located between the inlet and outlet thermocouples and I represents the electrical current which is measured at the rod´s circuit points. The power supply of the heating rod is a direct current voltage unit (Peak Tech L535). The electrical resistance of the heating rod depends on temperature therefore a 0.5 mm NiCr/Ni thermocouple is attached at the rod´s hot end. The measured rod temperature is used to calculate the electrical resistance.

2.2 Viscometer

The kinematic viscosity of the fluid is analyzed by a circular, capillary tube. The mass flux of a fluid in a circular tube depends on the pressure drop between the tube inlet and the tube outlet. Assuming that the fluid flow is laminar the relationship between mass flux and pressure drop is characterized by the Poiseuille equation as follows:

$$\nu = \frac{\Delta p \cdot \pi \cdot d^4}{128 \cdot \dot{m} \cdot l} \tag{3}$$

Here ν describes the kinematic viscosity, Δp is the measured pressure difference between two control points, d the inner diameter of the capillary, $\dot{m}$ is the mass flux of the fluid and l corresponds to the length of the capillary, i.e. the distance of the two pressure control points. To ensure that the flow within the capillary is laminar, the Reynolds number has to be checked whether it is below 2300. The Reynolds number is calculated as follows:

$$\mathrm{Re} = \frac{4 \cdot \dot{m}}{\pi \cdot d \cdot \rho \cdot \nu} \tag{4}$$

As shown from equation (4) the fluid density ρ and the kinematic viscosity ν are required. In the beginning these values are unknown. They have to be estimated for example by water data in the dedicated temperature and pressure range. The Reynolds number determines the upper limit of the mass flux. After measuring of kinematic viscosity and density, the mass flux has to be checked whether the flow condition was laminar. If not, the measurements have to be repeated with a lower mass flux.

The capillary tube is made of alloy 1.4571 and has an inner diameter of 4 mm. The total length of the capillary amounts to 1400 mm at which the first 501 mm are the inlet zone (l_{ein} in Figure 1) where the typical velocity profile of the Poisseuille flow is not fully developed. After the inlet zone the first pressure control point is located. The second one is 801 mm further downstream. Both control points are connected to a differential pressure manometer (Endress+Hauser PMD75), called PDI in Figure 1, which has an accuracy of 10^{-3} mbar. The capillary is aligned horizontal in order to avoid hydrostatic pressure differences and is surrounded by an electric heater and an insulation of 120 mm thickness to compensate for heat loss. Several thermocouples allow for controlling the temperature along the tube length which is kept constant by the electric heater. The mass flux is measured in the same way as it is described in section 2.1. The measurements are run as follows: First the capillary is filled with geothermal water at in-situ pressure and temperature. A constant mass flow is adjusted by the pressure retention valve V-12, shown in Figure 1. The heater of the capillary is switched on and controlled in order to keep the fluid temperature constant along the tube. Then the pressure difference is recorded, as well as the fluid temperature distribution along the tube and the entrance pressure (P1in Figure 1) for 5 to 15 minutes. The mass flux is determined by the continuous recording of the balance signal. Afterwards the fluid flow is interrupted by closing valve V-11 and the pressure difference is again recorded in order to detect the instrument offset. The difference of both, the PDI-signal at flow and at non-flow condition determines the effective pressure difference Δp which is required in equation (3).

2.3 Density Measuring Instrument

Due to the elevated fluid temperature one can hardly find an instrument which allows for the density determination of the saliferous and gaseous thermal water. Therefore an easy discontinuous measuring principle was chosen. A small pressure tank (called densimeter in Figure 1) with two tank inlets is installed in the mobile test facility, described in section 2.4. At both tank inlets, two blocking valves are fixed. The tank consist of stainless steel 1.4401 and can be filled with geothermal water under in-situ temperature and pressure conditions by connecting the mobile test plant to the geothermal pipe system. A thermocouple inside of the tank allows for temperature control. The pressure is measured at the tank entrance, P1 in Figure 1. The tank volume and the tank mass are well known. They amount to m=6846 g and V=1031 ml at 20°C. In addition, the tank is surrounded by an electric heater and an insulation which compensate for heat loss. After filling the tank with geothermal water and/or test fluids, in- and outlet valves are closed. The tank now contains a well-defined fluid volume. After removing the tank from the pipe system its mass is detected by weighting. The fluid density corresponds to the fluid mass per tank volume at the dedicated temperature and pressure. At higher fluid temperatures the tank is heated in order to keep the fluid temperature constant during filling and weighting. The volume of the steel tank changes with temperature due to the thermal expansion of the tank material. The change of tank volume as function of temperature is calculated by taking a coefficient of expansion of $17.5 \cdot 10^{-6}$ K^{-1} into account.

2.4 Mobile Test Facility

The measuring instruments, described above, are all installed in a mobile setup and connected by metal pipes. A scheme of the setup is shown in Figure 1.

The left part of Figure 1 (borehole simulation) is the stationary test section which remains in the laboratory. It is necessary to simulate the temperature and pressure conditions of geothermal water in the pipe system of geothermal power plants in the laboratory. Its main components are the fluid tank, the high pressure piston pump (Pu, Leva EK/2) and an oil bath heater (H). The sample fluid is filled into the tank. The fluid pressure is adjusted by the piston pump and the oil bath heater allows for measurements up to 170°C fluid temperature.

The mobile setup starts at valve V-1. If the measurements are made on site, a heated compression-proof flexible tube connects V-1 to the geothermal power plant pipe system. Entrance temperature and pressure of the mobile setup (TI 28 and P1) correspond to the fluid conditions in the geothermal power plant. They are controlled and kept constant by the heaters which are wrapped around the connecting pipes of the mobile setup. Fluid density can be measured by filling the densimeter with hot thermal water under pressure. If the valves V-3, V-4 and V-5 are closed the densimeter can be removed from the test plant for weighting. The determination of isobaric heat capacity and kinematic viscosity is performed alternatively by opening and closing valves V-6 and V-7. After passing the calorimeter or the viscometer the fluid is cooled to room temperature in the cooler K. With the help of a coriolis mass flow detector (F, Wagner, Mini Cori-Flow) the fluid mass flux can be measured in the high pressure part of the test facility where release of dissolved gases is suppressed. The system pressure is reduced by valve V-12 (Tescom, Serie 26-1700) and the fluid can be collected in a tank which is placed on a balance (Sartorius, LP34000P). The balance signal, i.e. the change of fluid mass by time, is recorded on a computer and allows for mass flux determination of the liquid fluid phase.

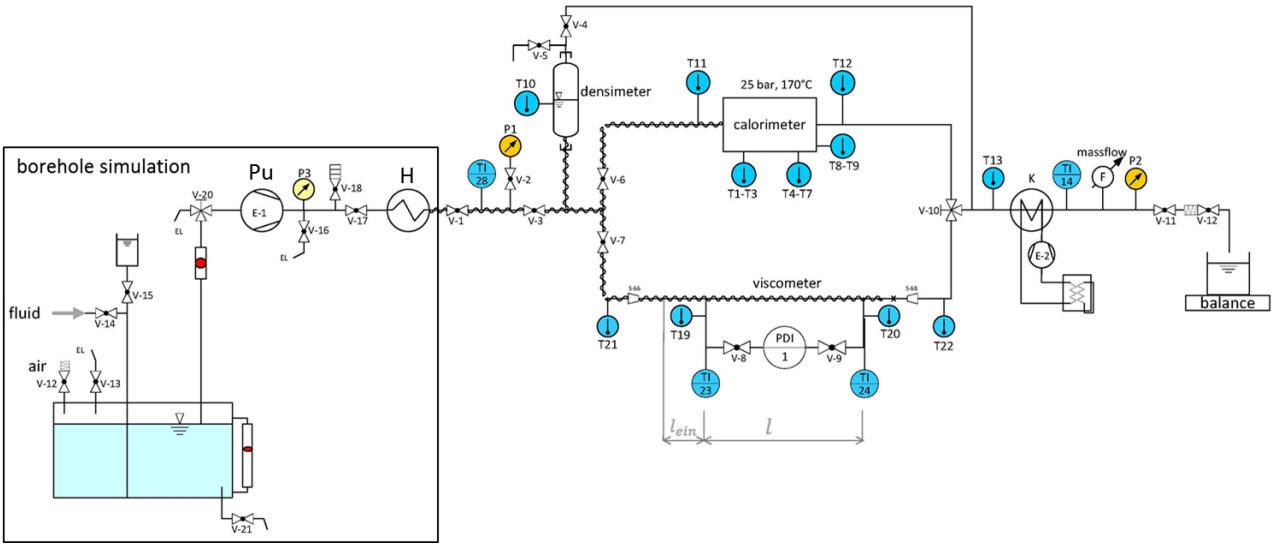

Figure 1: Connection scheme of the mobile measuring unit. Left part represents the borehole simulation devices which are necessary to test the mobile setup in the laboratory.

3. RESULTS

In order to test the measuring instruments, experiments with deionized and degassed water were made for different temperatures and pressures. Pressure and temperature were both measured at the entrance of each instrument. Literature data for isobaric heat capacity, kinematic viscosity and density are provided for comparison. Further, measurements of aqueous sodium chloride solutions are made. For this several solutions with different salt concentrations are mixed prior to the experiments. Aqueous sodium chloride solutions are chosen because a lot of literature data is available especially for isobaric heat capacity. Salt solutions are very corrosive particularly at temperature above 100°C. Therefore the instruments can be tested for their chemical resistance.

3.1 Isobaric Heat Capacity Measurements

3.1.1 Water Experiments

The measurements were run in the laboratory where the pressure and temperature conditions of a borehole were simulated, Figure 1. The entrance parameters of the fluid into the mobile setup like fluid pressure and fluid temperature were adjusted by the pressure piston pump (Pu) and the preheater (H), as shown in Figure 1. Both parameters were measured by the pressure sensor (P1) and the thermocouple (TI 28). For every preset fluid temperature controlled by (TI28), the heat capacity measurements were made several times at different power settings of the heating rod. This allows for testing, whether heating power and thus induced heat losses have an influence on the measurements. The standard deviation of the data was below 1% of the arithmetic mean. This error is shown in Figure 2 as vertical bars. The arithmetic means of the measurements are given as black dots in Figure 2 for different fluid entrance temperatures, measured by TI 28 (shown in Figure 1). Additionally values of the NIST database, Lemmon, et al. (2010), are added as continuous line. As shown from Figure 2, the relative error is around 1% based on the reference data. This accuracy is within the measuring error as reported in Picker, et al. (1971), Perron, et al. (1975) and Desnoyers, et al. (1976) who as well made experiments with flow calorimeters.

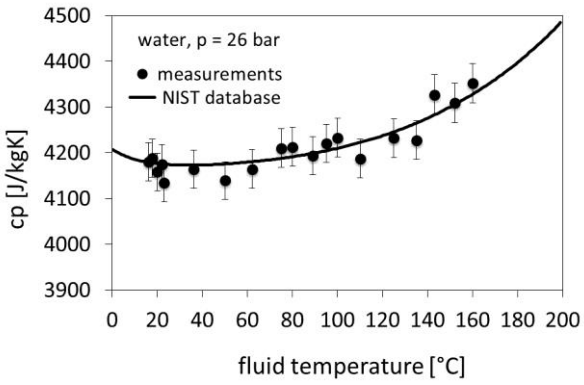

Figure 2: Isobaric heat capacity of deionized and degassed water at 26 bar and different temperatures. The solid line marks values of the NIST database, Lemmon, et al. (2010).

3.1.2 Aqueous Sodium Chloride Solutions

Heat capacity of aqueous sodium chloride solutions can be found in literature, e.g. in Thurmond and Brass (1988), Smith-Magowan and Wood (1981), Hnědkovský, et al. (2002), Picker, et al. (1971), Perron, et al. (1975) and Desnoyers, et al. (1976) for different temperatures and pressures. Many efforts on modelling heat capacity of salt solutions are made, e.g. in Archer (1992), Driesner (2007) and Gates, et al. (1987) but all of them need accurate information on the salt composition and concentration. Unfortunately multi component fluids are hardly modeled and only few data is available for aqueous solutions which contain different kinds of ions such as sodium, calcium, sulfate and carbonate. Based on well-known data of sodium chloride solutions the flow calorimeter is tested for its accuracy. For these measurements different salt concentrations, temperatures and pressures are adjusted, related to available reference data. The experimental results are shown in Figure 3. Reference data are taken from Smith-Magowan and Wood (1981), Sharqawy, et al. (2010), Hnědkovský, et al. (2002) and VDI-Wärmeatlas (2006).

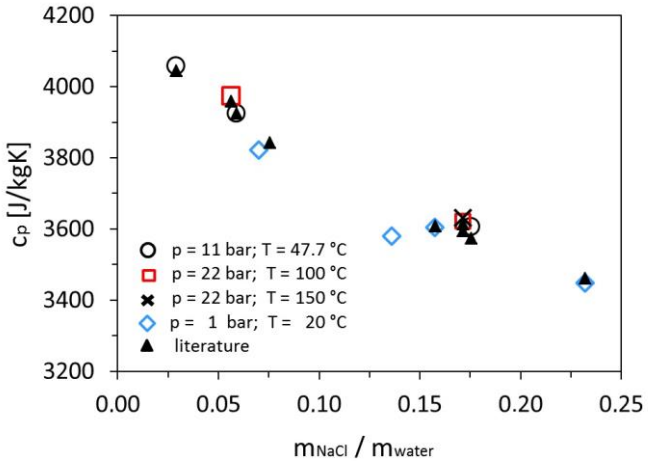

Figure 3: Isobaric heat capacity of aqueous sodium chloride solutions at different concentrations, temperatures and pressures. Corresponding literature data are taken from Smith-Magowan and Wood (1981), Sharqawy, et al. (2010), Hnědkovský, et al. (2002) and VDI-Wärmeatlas (2006).

As shown in Figure 3, increasing salt content leads to a significant decrease of heat capacity. Power plant dimensioning based on pure water data leads therefore to oversized power plant components, i.e. heat exchangers and thus to higher investment costs, as already mentioned before. The relative error between measured and reference data is within the error range of the water experiments and amounts to 1% of the reference data. Corrosion problems occurred at the heating rod, but could be eliminated by covering the heater with a thin, highly corrosion resistant metal capillary. Scaling could be removed by taking the probe heads out of the tube and cleaning. These salt experiments show that the flow calorimeter is suitable for being deployed under the rough conditions at geothermal sites and that the accuracy is within a range provided by other scientists, e.g. Thurmond and Brass (1988) and Sharqawy, et al. (2010).

3.2 Kinematic Viscosity Measurements

Dynamic and kinematic viscosities also influence geothermal power plant dimensioning but to a lower amount than isobaric heat capacity. Pressure drop of the fluid in the power plant pipe system which determines the pumping power of the feed and the reinjection pump is according to the fluid viscosity. Within the heat exchanger the dependence of heat transfer coefficient on fluid viscosity comes into consideration. Intensity of turbulence is determined by the kinematic viscosity. Heat transfer between fluid and heat exchanger wall is dominated by the intensity of turbulence, as described in VDI-Wärmeatlas (2006). Therefore imprecise data of fluid viscosity lead to imprecise determination of heat transfer within heat exchangers and further to imprecise determination of pumping power and thus efficiency of the power plant. For this a flow viscometer was built and tested in order to measure kinematic viscosity on site. Results of first laboratory experiments with water and salt solutions are shown in Figure 4.

3.2.1 Water Experiments

Experiments with deionized and degassed water were made for testing the accuracy of the instrument. The results are shown in Figure 4 for a fluid pressure of 26 bar and different fluid temperatures. Additionally, water data of the NIST database, Lemmon, et al. (2010), are added as solid line. As shown from Figure 4 the measured values agree quite well with the reference data. The relative error of the measured values is at most 3% of the reference data. The main influence on the precision of the viscometer is the uncertainty of the capillary diameter. High precision manufactured tubes will therefore enhance the accuracy of the measurements.

3.2.2 Aqueous Sodium Chloride Solutions

Experiments with sodium chloride solutions at salt content of $m_{NaCl} / m_{H20} = 0.165$ are made at a pressure of 22 bar (abs) and two temperatures, 100 °C and 150 °C. The results are shown in Figure 4 and marked by squares. The kinematic viscosity of the salt solution is higher than the kinematic viscosity of water. Thus pressure drop within the power plant components will be higher than estimated values which are based on water viscosities. In Figure 4 reference data of Kestin, et al. (1981b) are given for two different sodium chloride concentrations. The data are shown as dotted lines. The reference data correspond to lower pressures but nevertheless they can be compared to the own experimental data due to the fact that the pressure dependence of dynamic viscosity is minor important as reported in the article of Kestin, et al. (1981b).

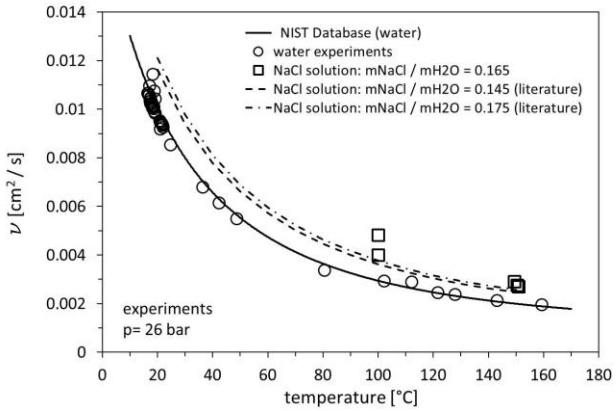

Figure 4: Kinematic viscosity of deionized and degassed water at 26 bar and different temperatures. Viscosities of NIST database are calculated at 26 bar. Squares symbolize experiments with sodium chloride solutions at 22 bar. Reference data of sodium chloride solutions (dotted lines) are from Kestin, et al. (1981b) at a pressure of 1 bar.

3.3 Density Measurements

The density measurements with deionized and degassed water are realized at different temperatures and pressures and are shown in Figure 5. The pressure is adjusted by the pressure piston pump (Pu) and the fluid temperature is regulated by the oil bath heater (H) of the stationary test section, Figure 1. The volume of the densimeter tank is determined by filling the tank with water under ambient conditions and measuring the water volume. This procedure was repeated several times and the arithmetic mean of the tank volume was identified to V=1031 ml with a precision of 0.1%. The tank mass amounts to m=6846 g and the accuracy of the mass corresponds to the accuracy of the balance i.e. 0.4%.

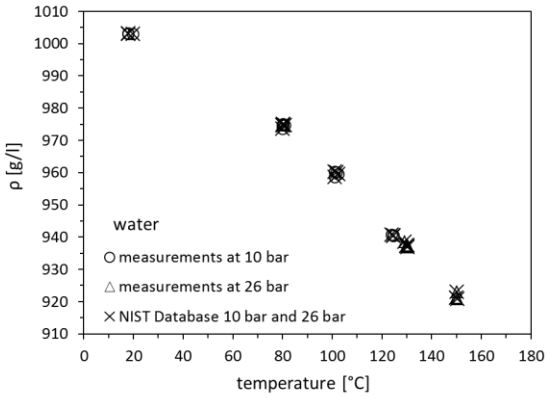

Figure 5: Density of deionized and degassed water at 26 bar and different temperatures. Reference data are from Lemmon, et al. (2010) at pressures of 10 bar and 26 bar.

The measured fluid densities are compared to the corresponding values of the NIST database, Lemmon, et al. (2010). Both data are given in Figure 5. The deviation of measured and reference data amounts to 0.4% based on reference data. Further experiments with aqueous sodium chloride solutions will be made in future work.

4. CONCLUSION

Measuring instruments for determination of physical fluid properties were designed, built and tested. In particular a flow calorimeter, a flow viscometer and a densimeter are arranged in a mobile setup for conducting measurements at geothermal sites. The maximum operating pressure of the instruments is about 30 bar and the operating temperature is limited to 170°C. This mobile setup will be connected to the geothermal pipe system for performing the measurements. The fluid properties like isobaric heat capacity, kinematic viscosity and density can be executed as single point or multi point measurement at varying temperatures and/or pressures by adjusting the pipe heating and by pressure regulation of the mobile setup. The instruments are tested in the laboratory at pressures up to 26 bar (abs) and temperatures of at most 165°C with deionized and degassed water and with aqueous sodium chloride solutions. The measured heat capacity differs to 1% from reference data. The relative error of the kinematic viscosity results is at most 3% based on literature data whereas the error of the density measurements amounts to 0.4%. Thus these instruments are a helpful tool to determine geothermal fluid properties at operating power plant conditions in order to allow for a better dimensioning of power plant components.

REFERENCES

Archer, D.G.: Thermodynamic Properties of the NaCl+H_2O System. II. Thermodynamic Properties of NaCl(Aq), NaCl*$2H_2O$(Cr), and Phase Equilibria, *Journal of Physical and Chemical Reference Data*, **21**, (1992), 793-829.

Desnoyers, J.E., Visser, C., Perron, G. and Picker, P.: Reexamination of the Heat Capacities Obtained by Flow Microcalorimetry. Recommendation for the Use of a Chemical Standard, *Journal of Solution Chemistry*, **5**, (1976), 605-616.

Driesner, T.: The System H_2O–Nacl. Part Ii: Correlations for Molar Volume, Enthalpy, and Isobaric Heat Capacity from 0 to 1000 °C, 1 to 5000 bar, and 0 to 1 mol X_{NaCl}, *Geochimica et Cosmochimica Acta*, **71**, (2007), 4902-4919.

Finger, J. and Blankenship, D.: Handbook of Best Practices for Geothermal Drilling, Sandia National Laboratories, Albuquerque, New Mexico 87185 and Livermore, California 94550, (2010).

Gates, J.A., Tillett, D.M., White, D.E. and Wood, R.H.: Apparent Molar Heat Capacities of Aqueous NaCl Solutions from 0.05 to 3.0 $mol \cdot kg^{-1}$, 350 to 600 K, and 2 to 18 MPa, *The Journal of Chemical Thermodynamics*, **19**, (1987), 131-146.

Hnědkovský, L., Hynek, V., Majer, V. and Wood, R.H.: A New Version of Differential Flow Heat Capacity Calorimeter; Tests of Heat Loss Corrections and Heat Capacities of Aqueous NaCl from T = 300 K to T = 623 K, *The Journal of Chemical Thermodynamics*, **34**, (2002), 755-782.

Kestin, J., Khalifa, H.E. and Correia, R.J.: Tables of the Dynamic and Kinematic Viscosity of Aqueous KCl Solutions in the Temperature Range 25-150 °C and the Pressure Range 0.1-35 MPa, *Journal of Physical and Chemical Reference Data*, **10**, (1981a), 57-70.

Kestin, J., Khalifa, H.E. and Correia, R.J.: Tables of the Dynamic and Kinematic Viscosity of Aqueous NaCl Solutions in the Temperature Range 20-150 °C and the Pressure Range 0.1-35 MPa, *Journal of Physical and Chemical Reference Data*, **10**, (1981b), 71-88.

Lemmon, E.W., Huber, M.L. and McLinden, M.O., Nist Reference Fluid Thermodynamic and Transport Properties—Refprop, in, Physical and Chemical Properties Division, National Institute of Standards and Technology, Boulder, Colorado 80305 U.S., 2010.

Perron, G., Fortier, J.-L. and Desnoyers, J.E.: The Apparent Molar Heat Capacities and Volumes of Aqueous NaCl from 0.01 to 3 mol kg^{-1} in the Temperature Range 274.65 to 318.15 K, *The Journal of Chemical Thermodynamics*, **7**, (1975), 1177-1184.

Perron, G., Roux, A. and Desnoyers, J.E.: Heat Capacities and Volumes of NaCl, $MgCl_2$, $CaCl_2$, and $NiCl_2$ up to 6 molal in Water, *Canadian Journal of Chemistry*, **59**, (1981), 3049-3054.

Picker, P., Leduc, P.-A., Philip, P.R. and Desnoyers, J.E.: Heat Capacity of Solutions by Flow Microcalorimetry, *The Journal of Chemical Thermodynamics*, **3**, (1971), 631-642.

Schröder, E., Neumaier, K., Nagel, F. and Vetter, C.: Study on Heat Transfer in Heat Exchangers for a New Supercritical Organic Rankine Cycle, *Heat Transfer Engineering*, **35**, (2014), 1505-1519.

Schröder, H., Teschner, M., Köhler, M., Seibt, A., Krüger, M., Friedrich, H.-J. and Wolfgramm, M., Long Term Reliability of Geothermal Plants – Examples from Germany, in: European Geothermal Congress 2007, Unterhaching, Germany, 2007.

Sharqawy, M.H.: New Correlations for Seawater and Pure Water Thermal Conductivity at Different Temperatures and Salinities, *Desalination*, **313**, (2013), 97-104.

Sharqawy, M.H., Lienhard V, J.H. and Zubair, S.M.: Thermophysical Properties of Seawater: A Review of Existing Correlations and Data, *Desalination and Water Treatment*, **16**, (2010), 354-380.

Smith-Magowan, D. and Wood, R.H.: Heat Capacity of Aqueous Sodium Chloride from 320 to 600 K Measured with a New Flow Calorimeter, *The Journal of Chemical Thermodynamics*, **13**, (1981), 1047-1073.

Thurmond, V.L. and Brass, G.W.: Activity and Osmotic Coefficients of Sodium Chloride in Concentrated Solutions from 0 to -40°C, *Journal of Chemical & Engineering Data*, **33**, (1988), 411-414.

VDI-Wärmeatlas: *10th ed. ed.*, VDI-Verlag, Düsseldorf, (2006).

Vetter, C., Wiemer, H.-J. and Kuhn, D.: Comparison of Sub- and Supercritical Organic Rankine Cycles for Power Generation from Low-Temperature/Low-Enthalpy Geothermal Wells, Considering Specific Net Power Output and Efficiency, *Applied Thermal Engineering*, **51**, (2013), 871 - 879.

Xu, T. and Pruess, K.: Thermophysical Properties of Sodium Nitrate and Sodium Chloride Solutions and Their Effects on Fluid Flow in Unsaturated Media, Lawrence Berkeley National Laboratory, University of California, Berkeley, CA 94720, (2001).